ARTICLES

Characterization of Fractions from Repeated Functionalization Reactions of Carbon Nanotubes

Yi Lin, Shelby Taylor, Weijie Huang, and Ya-Ping Sun*

Department of Chemistry and Center for Advanced Engineering Fibers and Films, Howard L. Hunter Chemistry Laboratory, Clemson University, Clemson, South Carolina 29634-0973

Received: March 13, 2002; In Final Form: September 13, 2002

The fractionation of a purified pristine multiple-walled carbon nanotube (MWNT) sample was achieved via repeated functionalization reactions to produce several soluble nanotube fractions. The reactions were based on the esterification of the nanotube-bound carboxylic acids. The soluble nanotube fractions and the insoluble solid residue were characterized by using optical spectroscopy, electron microscopy, and other techniques. The results show that all of these soluble samples contain primarily functionalized MWNTs and that there is little difference among these soluble nanotube fractions, either in the degree of nanotube dispersion or in the nanotube length and diameter distributions. There are apparently no preferential solubilization of carbon nanoparticles or other carbon impurities present in the starting nanotube sample and also no selectivity in the solubilization of MWNTs of different sizes (lengths and diameters) in the functionalization reactions. Mechanistic implications of the results are discussed.

Introduction

The chemical modification and solubilization of carbon nanotubes represent an emerging area in the research on nanotube-based materials. Several research groups have reported successful functionalization reactions for single-walled (SWNT) and multiple-walled (MWNT) carbon nanotubes.[1−14] These reactions may roughly be divided into two categories: the functionalization via a direct attachment to the graphitic surface and the functionalization via the use of intrinsic or induced (due to the shortening of the nanotubes,[15,16] for example) defects. For the former approach, Margrave, Smalley, and co-workers reported the fluorination of SWNTs.[2] In various alcohol solvents, these functionalized SWNTs were solvated as individual tubes, making it possible to carry out further solution chemistry. Pekker and co-workers reported the hydrogenation of carbon nanotubes via the Birch reduction in ammonia.[12] Other examples for the direct attachment of functional groups to the nanotube graphitic surface include the reports of Tour and co-workers on the derivatization of small-diameter (ca. 0.7 nm) SWNTs,[11] and the report of Wilson and co-workers on the functionalization and solubilization of SWNTs in reactions with anilines.[10]

The other category for the nanotube functionalization includes the reactions with the nanotube-bound carboxylic acids. Haddon and co-workers first reported the use of these acid groups for attaching long alkyl chains to SWNTs via amide linkages[1] or via carboxylate−ammonium salt ionic interactions.[8] Sun and co-workers showed that the esterification of the carboxylic acids can also be used to functionalize and solubilize nanotubes of any lengths.[4−6] An advantage with the ester linkages is that they can be easily defunctionalized via acid- or base-catalyzed hydrolysis, allowing the recovery of carbon nanotubes from the soluble samples.[6] In addition to long alkyl chains, polymeric systems have also been employed for the solubilization or dispersion of carbon nanotubes.[4,13,14,17−19] In particular, polymer-bound amino or hydroxy moieties have been used in the amidation and esterification reactions to attach the polymers to carbon nanotubes. Recently, Sun and co-workers reported the functionalization of both SWNTs and MWNTs with lipophilic and hydrophilic dendron species, which are more effective than simple long-chain alkyl functionalities for the solubilization of the nanotubes in organic solvents and water.[6a]

The solubilized carbon nanotube samples have allowed the fractionation and purification of the nanotubes in solution via techniques such as chromatography.[9] On the other hand, the functionalization itself may be used to fractionate nanotube samples. The results from such fractionation are particularly valuable to an evaluation of several important issues, including the selectivity of the functionalization reaction with respect to carbon nanotubes vs carbon impurities in the purified sample and the selectivity toward nanotubes of different sizes. Here we report the fractionation of a purified MWNT sample via repeated functionalization reactions. The results from characterization and analysis of the soluble fractions and the solid residue using spectroscopic, microscopic, and other techniques are presented and discussed.

Experimental Section

Materials. Methyl 3,5-dihydroxybenzoate (98%) was purchased from Avocado Research Chemicals, 1-bromohexadecane (99%) and thionyl chloride (99.5+%) from Acros, and lithium aluminum hydride ($LiAlH_4$) from Alfa Aesar. Solvent grade THF was first dried and distilled over molecular sieves, and

* Corresponding author.

10.1021/jp020701d CCC: $25.00 © 2003 American Chemical Society
Published on Web 01/07/2003

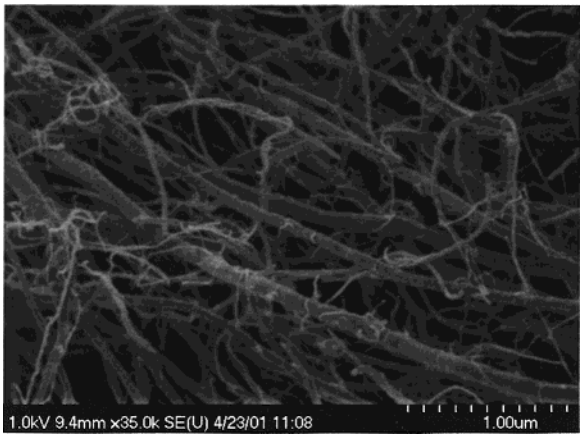

Figure 1. An SEM image of the purified pristine MWNT sample.

then distilled over sodium before use. Other solvents were either of spectrophotometry/HPLC grade or purified via simple distillation. Deuterated NMR solvents were obtained from Cambridge Isotope Laboratories.

The MWNT sample, produced via the chemical vapor deposition (CVD, or sometime called catalytic pyrolysis) method using xylene as precursor and ferrocene as catalyst,[20,21] was supplied by Professor A. M. Rao of the Physics Department, Clemson University. The SEM analysis of the as-produced nanotube sample showed that it contained predominantly MWNTs, with only a small quantity of iron and iron oxide particles (from the catalyst).[22] The result is consistent with the conclusion in the literature that nanotube samples produced via the CVD method are hardly contaminated with amorphous carbon and carbon nanoparticles.[20,21] For the purification to remove iron-containing impurities,[22] the MWNT sample was heated and stirred in an aqueous HNO_3 solution (2.6 M) for 2 days. Upon vigorously centrifuging the suspension, the solid sample was washed repeatedly with deionized water and then dried under vacuum. For quality control, the purified MWNT sample was characterized by TGA, Raman, and SEM. The results indicate that the nanotube sample used in the functionalization reactions is best described as a mixture of MWNTs of different lengths (as long as a few microns) and different diameters (up to ~150 nm). A typical SEM image of the purified MWNT sample is shown in Figure 1.

Measurements. ^{1}H and ^{13}C NMR spectra were obtained on a Bruker AC-300 NMR spectrometer and a JEOL Eclipse +500 NMR spectrometer. Tetramethylsilane was used as an internal standard. Absorption spectra were obtained using a computer-controlled Shimadzu UV2101-PC spectrophotometer. Raman spectra were recorded on a Renishaw Raman spectrometer equipped with a 780 nm solid-state laser source of 50-mW maximum output. Thermal gravimetric analysis (TGA) was carried out on a Mettler-Toledo TGA/SDTA851 system. Scanning electron microscopy (SEM) imaging was performed on a Hitachi 4700 field-emission SEM system with the energy-dispersive X-ray analysis capability. A specimen for SEM analysis was prepared by placing a solid-state sample directly onto a carbon tape on top of an aluminum stub. Transmission electron microscopy (TEM) images were obtained on a Hitachi S7000 TEM system operated at an acceleration voltage of 125 kV. A specimen for TEM imaging was prepared by applying a few drops of the nanotube solution under consideration onto a carbon-coated copper grid and then evaporating off the solvent.

Dendron I. Methyl 3,5-dihexadecoxybenzoate (8 g, 13 mmol), which was obtained from the etherification of methyl 3,5-dihydroxybenzoate and 1-bromohexadecane (97% yield), was dissolved in diethyl ether (250 mL), and to the solution was added $LiAlH_4$ (0.54 g, 14.3 mmol). The mixture was refluxed under nitrogen protection for 12 h. Upon the completion of the reduction reaction, water was added carefully to quench the unreacted $LiAlH_4$. Dendron **I** was extracted from the reaction mixture with diethyl ether and recovered as a colorless compound (96% yield). ^{1}H NMR (300 MHz, $CDCl_3$): $\delta = 0.88$ (t, $J = 6.6$ Hz, 6H), 1.26−1.55 (m, 52H), 1.71−1.79 (m, 4H), 3.93 (t, $J = 6.6$ Hz, 4H), 4.62 (d, $J = 3.0$ Hz, 2H), 6.38 (t, $J = 2.2$ Hz, 1H), 6.50 (d, $J = 2.2$ Hz, 2H) ppm. ^{13}C NMR (75 MHz, $CDCl_3$): $\delta = 14.34$, 22.92, 26.27, 29.48, 29.60, 29.91, 32.15, 65.71, 68.28, 100.76, 105.25, 143.40, 160.75 ppm. MS (EI+): 589 (588 + 1). mp (DSC): 36 °C.

Functionalization of Carbon Nanotubes. In a typical reaction, a purified MWNT sample (47.2 mg) was refluxed with thionyl chloride (5 mL) at 70 °C under nitrogen protection for 24 h to convert the carboxylic acids into acyl chlorides. After a complete removal of residual thionyl chloride on a rotary evaporator, the sample was well mixed with carefully dried dendron **I** (487 mg, 0.84 mmol) in a flask, heated to 80 °C, and vigorously stirred for 24 h under nitrogen protection. The reaction mixture was repeatedly extracted with THF and chloroform to yield a colored solution. In the extractions, the solid residue was removed via centrifuging at a high speed (7800 rpm). The solution was concentrated for precipitation into ethanol (to remove unreacted **I** and other small molecules),[3,6a] yielding the functionalized nanotube sample **I-MWNT** as dark-colored solids.

The insoluble residue of the reaction mixture contained primarily unfunctionalized and under-functionalized MWNTs. This insoluble sample was used as the starting material in a repeat of the functionalization reaction with **I** for a second fraction. The same process was repeated for the third and fourth times to yield the corresponding fractions.

Results and Discussion

The solubilization of carbon nanotubes via functionalization has been reported by several research groups, as discussed in the Introduction. However, the notion that carbon nanotubes are actually functionalized to become soluble in a variety of solvents is hardly unanimously accepted. An important issue generally behind the questioning of the reported functionalization is associated with the fact that carbon nanotube samples almost always contain carbon nanoparticles and other carbon impurities. In particular, it has been a concern that the soluble sample might be largely due to the functionalization of carbon nanoparticles and impurities, namely that those species might be preferentially solubilized in the functionalization reactions. Thus, the fractionation via repeated functionalization reactions of the same nanotube sample provides an opportunity for a critical evaluation of the issue.

In this study, a MWNT sample produced by use of the CVD method was selected for the reactions because such a sample is known to contain relatively smaller amounts of carbon nanoparticles and other carbon impurities (Figure 1).[20,21] The functionalization reaction of purified MWNTs with dendron **I** yielded a dark-colored sample, designated as **I-MWNT-1**, which is soluble in common organic solvents such as chloroform, THF, toluene, etc. (requiring no sonication). The UV/vis absorption spectrum of the sample solution is shown in Figure 2. The spectrum is a featureless curve, typical for soluble functionalized carbon nanotubes.[6] The lack of structures in the absorption spectrum is likely due to the fact that it consists of contributions from a broad distribution of electronic transitions, which are

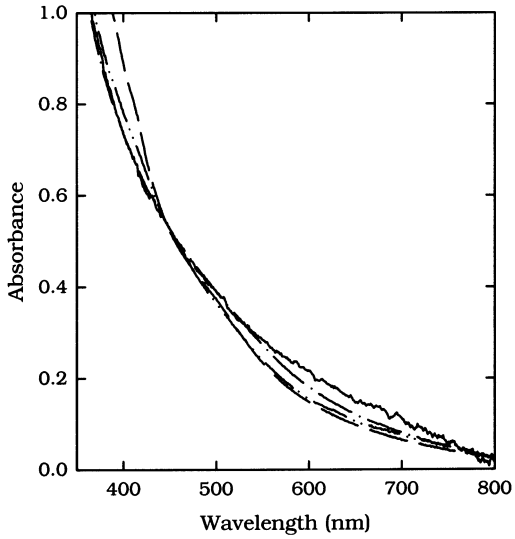

Figure 2. UV/vis absorption spectra (normalized) of soluble fractions **I-MWNT-*i*** in room-temperature chloroform solutions (corresponding to concentrations on the order of 0.5 mg/mL in 1-cm square cuvette): $i = 1$ (——), $i = 2$ (– – –), $i = 3$ (–•–•–), and $i = 4$ (–••–••–).

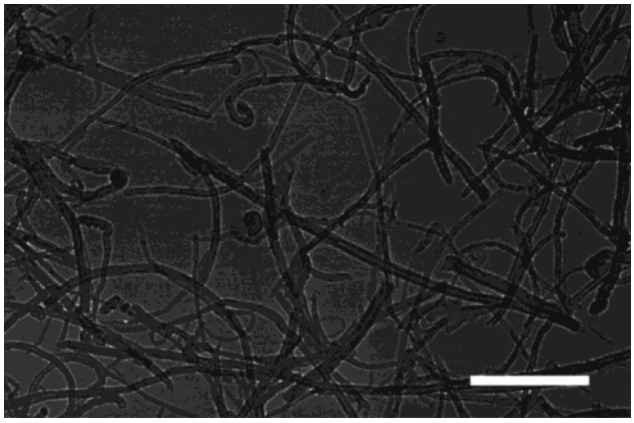

Figure 3. A TEM image of **I-MWNT-1** deposited on a carbon-coated copper grid (scale bar = 400 nm).

associated with functionalized MWNTs of different diameters and lengths and perhaps also varying surface properties. The solution was used to prepare a solid sample on a carbon-coated copper grid for TEM analyses. The TEM results clearly show that the soluble sample is dominated by functionalized MWNTs of different lengths and diameters (Figure 3) and that there is no evidence for any preferential solubilization of other carbon species.

The functionalization reaction was not complete, left behind a substantial amount of insoluble MWNTs (residue 42.5 mg), some of which might contain functional groups but not enough to become soluble.[23] The insoluble nanotube sample was then used as the starting material for a second round of functionalization reactions under the same experimental conditions. The soluble sample thus obtained is designated as **I-MWNT-2**. Again the reaction was not complete (residue 39.1 mg), allowing additional rounds of functionalization reactions to yield **I-MWNT-3** (residue 36.1 mg), and then **I-MWNT-4** (residue 21.3 mg). On the basis of the weight of the final residual insoluble sample, the four repeats of the functionalization reaction solubilized ~55% of the starting MWNTs. This estimate represents the lower limit because the residual insoluble sample also contains some functional groups that are probably associated with partially functionalized MWNTs (see below). All of

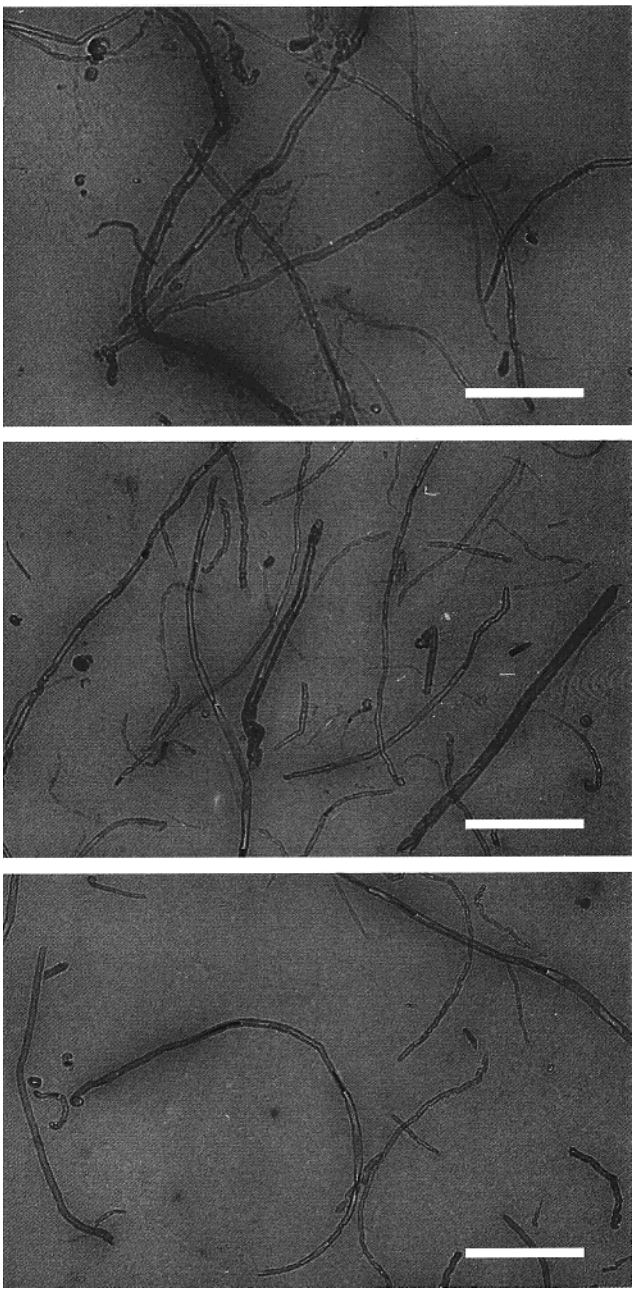

Figure 4. A comparison of TEM images of the soluble fractions **I-MWNT-*i***: $i = 2$ (top), $i = 3$ (middle), and $i = 4$ (bottom). All scale bars represent 400 nm.

the soluble samples are dark colored. Their UV/vis absorption spectra in room-temperature chloroform solutions are rather similar, as compared in Figure 2.

The soluble fractions **I-MWNT-*i*** ($i = 2, 3, 4$) on carbon-coated copper grids were also analyzed by TEM. A comparison of typical TEM images is provided in Figure 4. The results again show that these soluble samples contain functionalized MWNTs of different lengths and diameters. There is little difference among these soluble samples, either in the degree of nanotube dispersion or in the nanotube length and diameter distributions (Table 1). Such a lack of selectivity in the functionalization and solubilization of MWNTs of different sizes (lengths and diameters) is rather interesting, probably a reflection of some fundamental principles that dictate the solubilization of nanotubes via attaching highly soluble functional groups. Smaller and shorter nanotubes might be considered as easier targets in the solubilization because they should require relatively fewer

TABLE 1: Statistics of the Functionalized MWNTs[a]

	length (nm)		diameter (nm)		aspect ratio	
fraction	L_0 [b]	ΔL [c]	d_0 [b]	Δd [c]	R_0 [b]	ΔR [c]
1	167 ± 10	177	6.7 ± 0.5	5.5	22 ± 1	19
2	214 ± 23	216	10 ± 0.6	4.6	31 ± 3	27
3	206 ± 10	236	13.5 ± 1	9.9	14 ± 1	14
4	231 ± 12	165	13 ± 0.4	5.9	16 ± 1	11

[a] The results from the TEM images (on average 150 nanotubes) are best fitted empirically by using the log−normal distribution function: $f = a \exp\{-(1/2)[\ln(x/x_0)/b]^2\}$($x_0 = L_0$, d_0, or R_0). [b] The value corresponds to the peak of the log−normal distribution curve. [c] One-half of fwhm (full width at half-maximum) of the log−normal distribution curve.

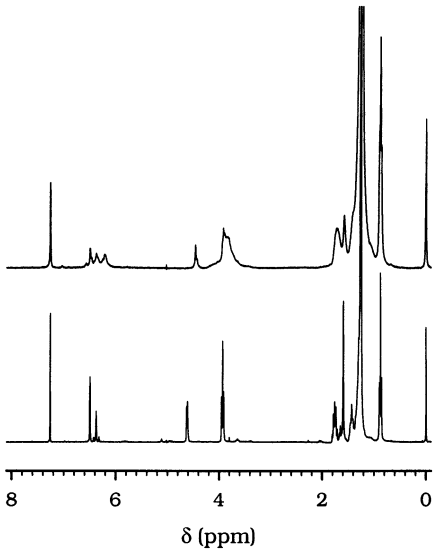

Figure 5. ^{1}H NMR spectra of **I** (bottom) and **I-MWNT-2** (top) in $CDCl_3$.

attached functional groups for the solubility. On the other hand, these nanotubes might contain fewer defect sites and the associated carboxylic acids, making it more difficult to attach a sufficient number of functional groups that are required for the solubility. Thus, on balance the smaller and shorter nanotubes are not necessarily preferred in the solubilization. The same rationalization may be applied to the results that show no preferential solubilization of carbon nanoparticles because these particles may conceptually be considered as the extremes of the smaller and shorter nanotubes. Simplistically, the selectivity or the lack of selectivity in the solubilization of nanotubes of different sizes is probably dictated by the density of the nanotube-bound carboxylic acids, or roughly the ratio between the number of acid groups and the number of carbons on a nanotube. A higher density of the acids allows the attachment of more functional groups per unit weight of a nanotube and consequently easier solubilization of the nanotube. In reality, however, the nanotube solubilization is likely more complicated. Many other factors, such as the shape and aspect ratio of a nanotube, may also contribute significantly to determine the solubility of the functionalized nanotube.

The solubility of the functionalized nanotube samples allowed NMR characterizations in solution. The ^{1}H NMR spectra of the **I-MWNT-*i*** samples are all similar, exhibiting broad signals at similar chemical shifts to those in the spectrum of **I**. Shown in Figure 5 is a comparison of the spectra of **I** and **I-MWNT-2**. The signals in both spectra are due to the protons in **I**, before and after being attached to nanotubes. The broad NMR signals are typical of protons in nanotube-bound functional groups.[6a]

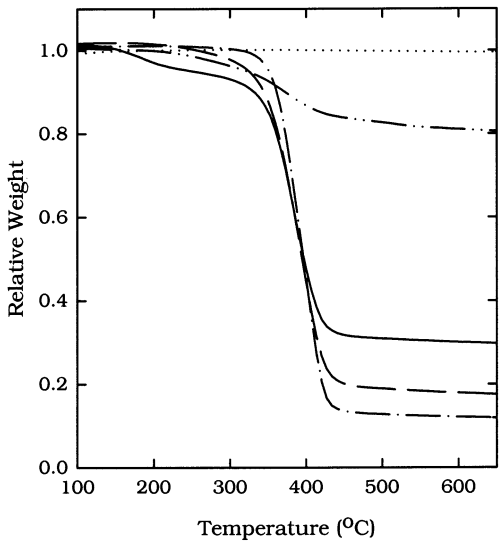

Figure 6. TGA (10 °C/min scanning rate and nitrogen atmosphere) traces of the purified pristine MWNT sample (···), the final residual insoluble sample (−··−··−), and the soluble fractions **I-MWNT-*i***: $i = 2$ (−·−·−), $i = 3$ (− − −), and $i = 4$ (——).

According to the results reported previously from measurements of the nuclei spin−lattice (T_1) and spin−spin (T_2) relaxation times,[6a] the signal broadening is likely due to the functionalized nanotubes being high molecular weight species of low mobility, similar to the broadening effects in NMR spectra of known polymeric systems.[24]

The solid-state samples of the soluble **I-MWNT-*i*** fractions were analyzed by TGA. The experiments were carried out in nitrogen atmosphere with a heating rate of 10 °C/min. The results show that the functionalized nanotubes undergo thermal defunctionalization under the TGA conditions. On the other hand, there is no meaningful weight loss for the purified pristine MWNT sample below ~700 °C. Thus, the weight loss as a result of thermal defunctionalization for the functionalized nanotube samples may be used to estimate the nanotube contents in these samples. Shown in Figure 6 are TGA traces of the soluble fractions **I-MWNT-*i*** ($i = 2$, 3, 4) in reference to that of the purified pristine MWNT sample. According to the residual sample weights at 650 °C, the estimated nanotube contents in the soluble fractions **I-MWNT-*i*** of $i = 2$, 3, and 4 are 13%, 20%, and 30%, respectively.[23] These are obviously rough estimates because of several possible interferences. For example, some of the functional groups may be trapped by the nanotubes in the solid state, despite the slow temperature scanning rate. The tendency for the defunctionalized nanotubes to aggregate may also contribute to the trapping of functional groups in the residual samples. Nevertheless, the estimates for the different soluble fractions are probably meaningful in a relative sense, namely that the trend of increasing nanotube contents in later fractions is likely real. This is consistent with a general observation in the nanotube functionalization reactions carried out in our laboratory that solubilizing a residual insoluble nanotube sample from a functionalization reaction is typically easier than solubilizing a purified pristine nanotube sample. An explanation for the observation might be that the residual insoluble nanotube sample contains under-functionalized nanotubes, which are MWNTs not sufficiently functionalized to become soluble. These nanotubes are better dispersed than purified pristine nanotubes because of the partial functionalization, making it more efficient for them to participate in subsequent functionalization reactions.

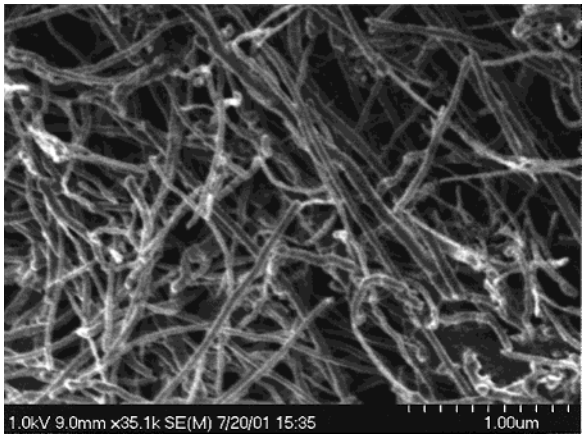

Figure 7. An SEM image of the final residual insoluble sample.

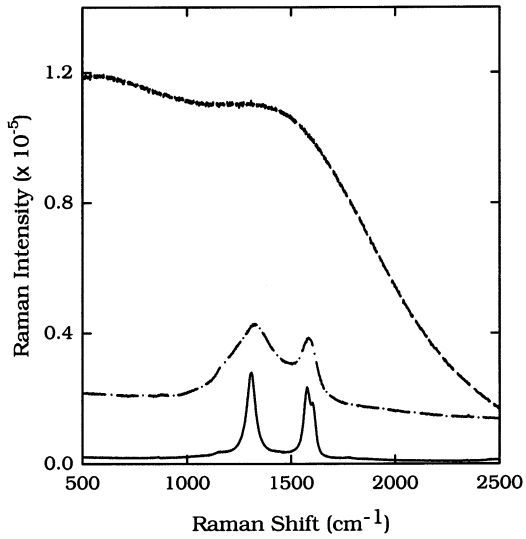

Figure 8. Raman spectra of **I-MWNT-3** before (− − −) and after thermal defunctionalization in a TGA scan to 650 °C (−·−·−). The spectrum of the purified pristine MWNT sample (——) is also shown for comparison.

An analysis of the final residual insoluble sample after the four repeated functionalization reactions yielded results that are supportive of the rationalization discussed above. The TGA trace of the sample measured under the same experimental conditions (10 °C/min in nitrogen atmosphere) is also shown in Figure 6. The weight loss of ∼20% may be attributed to the thermal defunctionalization and evaporation of the functional groups from the partially functionalized MWNTs. This can be used as a correction to the gravimetric estimate described above concerning the amount of MWNTs being functionalized and solubilized in the repeated reactions. Thus, the correct gravimetric estimate should be that ∼64% or more (if there are still functional groups in the post-TGA sample) of the starting MWNTs were solubilized in four sequential functionalization reactions.

The final residual insoluble sample was also analyzed by SEM and Raman. As shown in Figure 7, the SEM image confirms that the residual sample contains primarily MWNTs. The SEM results show no significant differences in nanotube sizes between the starting purified nanotube sample and the residual insoluble nanotube sample. This is in agreement with the conclusion discussed above that there are no significant selectivities in the functionalization reactions of MWNTs with dendron **I**. During the SEM analysis of the residual sample conducted at 1.0 kV, however, significant surface charging effects were observed.[25] The effects might be due to the presence of nonconductive species in the sample for analysis, consistent with the TGA result that the residual insoluble nanotube sample contains a significant amount (∼20% according to TGA) of functional groups. Because of the presence of partially functionalized MWNTs, the Raman measurement of the residual insoluble sample was subject to luminescence interference.[4] The Raman spectrum exhibits the characteristic tangential-mode peak of carbon nanotubes[20] on top of the luminescence background.

The luminescence interference became overwhelming in Raman measurements of the soluble fractions **I-MWNT-*i***, even with near-infrared excitation. As shown in Figure 8, for example, the Raman spectrum of **I-MWNT-3** (780 nm excitation) is essentially a luminescence spectrum. Since the luminescence is strongly dependent on the functionalization, it can be suppressed in defunctionalized nanotube samples.[4] Thus, the soluble fraction **I-MWNT-3** was thermally defunctionalized in a TGA scan to 650 °C. The Raman spectrum of the post-TGA sample is also shown in Figure 8. The Raman peaks, though broader, are comparable to those of the purified pristine MWNT sample (Figure 8).[20] The Raman results confirm again that the soluble fractions **I-MWNT-*i*** contain functionalized carbon nanotubes.

In summary, the fractions from repeated functionalization reactions of a MWNT sample were characterized. The results show that all of these soluble samples contain primarily functionalized MWNTs and that there are no preferential solubilization of carbon nanoparticles in the starting nanotube sample and also no selectivity in the solubilization of MWNTs of different sizes (lengths and diameters).

Acknowledgment. We thank Prof. A. M. Rao for supplying the MWNT sample and D. Hill for experimental assistance. Financial support from NSF (CHE-9727506 and, in part, EPS-9977797), NASA (NCC1-01036, NGT1-52238, and NAT1-01036), the South Carolina Space Grant Consortium, and the Center for Advanced Engineering Fibers and Films (NSF-ERC at Clemson University) is gratefully acknowledged.

References and Notes

(1) Chen, J.; Hamon, M. A.; Hu, H.; Chen, Y.; Rao, A. M.; Eklund, P. C.; Haddon, R. C. *Science* **1998**, *282*, 95.

(2) Mickelson, E. T.; Chiang, I. W.; Zimmerman, J. L.; Boul, P. J.; Lozano, J.; Liu, J.; Smalley, R. E.; Hauge, R. H.; Margrave, J. L. *J. Phys. Chem. B* **1999**, *103*, 4318. (b) Boul, P. J.; Liu, J.; Mickelson, E. T.; Huffman, C. B.; Ericson, L. M.; Chiang, I. W.; Smith, K. A.; Colbert, D. T.; Hauge, R. H.; Margrave, J. L.; Smalley, R. E. *Chem. Phys. Lett.* **1999**, *310*, 367.

(3) (a) Hamon, M. A.; Chen, J.; Hu, H.; Chen, Y.; Itkis, M. E.; Rao, A. M.; Eklund, P. C.; Haddon, R. C. *Adv. Mater.* **1999**, *11*, 834. (b) Niyogi, S.; Hu, H.; Hamon, M. A.; Bhowmik, P.; Zhao, B.; Rozenzhak, S. M.; Chen, J.; Itkis, M. E.; Meier, M. S.; Haddon, R. C. *J. Am. Chem. Soc.* **2001**, *123*, 733.

(4) (a) Riggs, J. E.; Guo, Z.; Carroll, D. L.; Sun, Y.-P. *J. Am. Chem. Soc.* **2000**, *122*, 5879. (b) Sun, Y.-P.; Martin, R. B.; Lin, Y.; Fu, K., manuscript in preparation.

(5) Riggs, J. E.; Walker, D. B.; Carroll, D. L.; Sun, Y.-P. *J. Phys. Chem. B* **2000**, *104*, 7071.

(6) (a) Sun, Y.-P.; Huang, W.; Lin, Y.; Fu, K.; Kitaygorodskiy, A.; Riddle, L. A.; Yu, Y. J.; Carroll, D. L. *Chem. Mater.* **2001**, *13*, 2864. (b) Fu, K.; Huang, W.; Lin, Y.; Riddle, L. A.; Carroll, D. L.; Sun, Y.-P. *Nano Lett.* **2001**, *1*, 439.

(7) Jin, Z.; Sun, X.; Xu, G.; Goh, S. H.; Ji, W. *Chem. Phys. Lett*. **2000**, *318*, 505.

(8) Chen, J.; Rao, A. M.; Lyuksyutov, S.; Itkis, M. E.; Hamon, M. A.; Hu, H.; Cohn, R. W.; Eklund, P. C.; Colbert, D. T.; Smalley, R. E.; Haddon, R. C. *J. Phys. Chem. B* **2001**, *105*, 2525.

(9) (a) Niyogi, S.; Hu, H.; Hamon, M. A.; Bhowmik, P.; Zhao, B.; Rozenzhak, S. M.; Chen, J.; Itkis, M. E.; Meier, M. S.; Haddon, R. C. *J. Am. Chem. Soc.* **2001**, *123*, 733. (b) Zhao, B.; Hu, H.; Niyogi, S.; Itkis, M. E.; Hamon, M. A.; Bhowmik, P.; Meier, M. S.; Haddon, R. C. *J. Am. Chem. Soc*. **2001**, *123*, 11673.

(10) Sun, Y.; Wilson, S. R.; Schuster, D. I. *J. Am. Chem. Soc.* **2001**, *123*, 5348.

(11) (a) Bahr, J. L.; Yang, J. P.; Kosynkin, D. V.; Bronikowski, M. J.; Smalley, R. E.; Tour, J. M. *J. Am. Chem. Soc.* **2001**, *123*, 6536. (b) Bahr, J. L.; Tour, J. M. *Chem. Mater.* **2001**, *13*, 3823.

(12) Pekker, S.; Salvetat, J.-P.; Jakab, E.; Bonard, J.-M.; Forró, L. *J. Phys. Chem. B* **2001**, *105*, 7938.

(13) Czerw, R.; Guo, Z.; Ajayan, P. M.; Sun, Y.-P. Carroll, D. L. *Nano Lett.* **2001**, *1*, 423.

(14) (a) Lin, Y.; Rao, A. M.; Sadanadan, B.; Kenik, E. A.; Sun, Y.-P. *J. Phys. Chem. B* **2002**, *106*, 1294. (b) Huang, W.; Lin, Y.; Taylor, S.; Gaillard, J.; Rao, A. M.; Sun, Y.-P. *Nano Lett.* **2002**, *2*, 231.

(15) Liu, J.; Rinzler, A. G.; Dai, H. J.; Hafner, J. H.; Bradley, R. K.; Boul, P. J.; Lu, A.; Iverson, T.; Shelimov, K.; Huffman, C. B.; Rodriguez-Macias, F.; Shon, Y. S.; Lee, T. R.; Colbert, D. T.; Smalley, R. E. *Science* **1998**, *280*, 1253.

(16) Hamon, M. A.; Hu, H.; Bhowmik, P.; Niyogi, S.; Zhao, B.; Itkis, M. E. Haddon, R. C. *Chem. Phys. Lett.* **2001**, *347*, 8.

(17) Koshio, A.; Yudasaka, M.; Zhang, M.; Iijima, S. *Nano Lett.* **2001**, *1*, 361.

(18) Tang, B. Z.; Xu, H. *Macromolecules* **1999**, *32*, 2569.

(19) Star, A.; Stoddart, J. F.; Steuerman, D.; Diehl, M.; Boukai, A.; Wong, E. W.; Yang, X.; Chung, S. W.; Choi, H.; Heath, J. R. *Angew. Chem., Int. Ed. Engl.* **2001**, *40*, 1721.

(20) (a) Andrews, R.; Jacques, D.; Rao, A. M.; Derbyshire, F.; Qian, D.; Fan, X.; Dickey, E. C.; Chen, J. *Chem. Phys. Lett.* **1999**, *303*, 467. (b) Rao, A. M.; Jacques, D.; Haddon, R. C.; Zhu, W.; Bower, C.; Jin, S. *Appl. Phys. Lett.* **2000**, *76*, 3813.

(21) Bulusheva, L. G.; Okotrub, A. V.; Asanov, I. P.; Fonseca, A.; Nagy, J. B. *J. Phys. Chem. B* **2001**, *105*, 4853.

(22) The purified MWNT sample may still contain a small amount of iron-related particles, but there is no evidence for any effects of these particles on the functionalization reactions.

(23) For all fractions, the apparent weight loss in the functionalization reaction underestimates the amount of MWNTs in the soluble sample in comparison with the result from the TGA analysis, because the residue from the reaction contains some functional groups.

(24) (a) Bloembergen, N.; Purcell, E. M.; Pound, R. V. *Phys. Rev.* **1948**, *73*, 679. (b) Swiff, T. J. *NMR of Paramagnetic Molecules*; La Mar, G. N., Horrocks, W. D., Jr., Holm, R. H., Eds.; Academic Press: New York and London, 1973.

(25) Surface charging effect in SEM analysis occurs when the sample surface is of low conductivity.[26] The effect is usually reduced significantly via coating the sample with a thin layer of metal, such as Pt or Au.

(26) Goldstein, J. I.; Newbury, D. E.; Echlin, P.; Joy, D. C.; Romig, A. D.; Lyman, C. E.; Fiori, C.; Lifshin, E. *Scanning Electron Microscopy and X-ray Microanalysis: A Text for Biologists, Materials Scientists, and Geologists*, 2nd ed.; Plenum Press: New York, 1992.